Forest Ecology and Management 523 (2022) 120487

Contents lists available at ScienceDirect

Forest Ecology and Management

journal homepage: www.elsevier.com/locate/foreco

Conifer seedling demography reveals mechanisms of initial forest resilience to wildfires in the northern Rocky Mountains

Kyra Clark-Wolf *, Philip E. Higuera, Kimberley T. Davis

Department of Ecosystem and Conservation Sciences, University of Montana, 32 Campus Drive, Missoula, MT 59812-0004, United States

ARTICLE INFO

Keywords:
Plant demography
Tree regeneration
Fire severity
Microclimate
Soil nitrogen
Climate change

ABSTRACT

Climate warming and an increased frequency and severity of wildfires are expected to transform forest ecosystems, in part through altered post-fire vegetation trajectories. Such a loss of forest resilience to wildfires arises due to a failure to pass though one or more critical demographic stages, or "filters," including seed availability, germination, establishment, and survival. Here we quantify the relative influence of microclimate and microsite conditions on key stages of post-fire seedling demography in two large, lightning-ignited wildfires from the regionally extensive fire season of 2017 in the northern Rocky Mountains, U.S.A. We tracked conifer seedling density, survival, and growth in the first three years post-fire in 69 plots spanning gradients in fire severity, topography, and climate; all plots were limited to within 100 m of a seed source to assure seed availability. Microclimate conditions were inferred based on measurements in a subset of 46 plots. We found abundant post-fire conifer regeneration, with a median of 2,633 seedlings per hectare after three years, highlighting early resilience to wildfire. This robust regeneration was due in part to moderate post-fire climate conditions, supporting high survivorship (>50% on average) of all seedlings tracked over the study period (n = 763). A statistical model based on variables describing potential seed availability, microclimate, fire severity, understory vegetation, and soil nitrogen availability explained 75% of the variability in seedling density among plots. This analysis highlights the overarching importance of fine-scale heterogeneity in fire effects, which determine microclimate conditions and create diverse microsites for seedlings, ultimately facilitating post-fire tree regeneration. Our study elucidates mechanisms of forest resilience to wildfires and demonstrates the utility of a demographic perspective for anticipating forest responses to future wildfires under changing environmental conditions.

1. Introduction

Forest ecosystems and the services they provide are changing due to the combined impacts of warmer, drier climate conditions and increased wildfire frequency and severity, driven strongly by anthropogenic climate change (Abatzoglou and Williams, 2016, Holden et al., 2018, Parks and Abatzoglou, 2020). These changes stem in part from altered patterns of post-fire tree regeneration, which is a critical stage of community re-organization affecting forest composition and structure for decades to centuries (Tepley et al., 2013, Turner et al., 2016). Across western North America, numerous studies document a decline in post-fire tree regeneration in the 21st century (e.g., Stevens-Rumann et al., 2018, Turner et al., 2019, Coop et al., 2020), a trend expected to continue under climate warming (Kemp et al., 2019, Davis et al., 2020). These changes can indicate a loss of resilience to wildfire, used here to reflect the capacity of an ecosystem to recover following a disturbance and retain fundamental structures and functions (Gunderson, 2000). Forest resilience to wildfire is ultimately governed by complex interactions among climate, disturbance regimes, and species-specific responses to biophysical conditions (e.g., Rammer et al., 2021). Ongoing warming and increasing fire activity highlight the pressing need to understand mechanisms of forest resilience to wildfires, how these mechanisms vary among species and across biophysical gradients, and if, when, and where forest resilience to wildfire will be overcome in the future.

Anticipating forest resilience to wildfires is aided by considering key demographic filters that control fire-caused tree mortality and post-fire tree regeneration (Davis et al., 2018). Tree regeneration is the net result of mechanisms influencing seed production and dispersal, and seedling germination, establishment, and survival over multiple years after a fire

* Corresponding author.
E-mail address: Kyra.Clark-Wolf@umontana.edu (K. Clark-Wolf).

https://doi.org/10.1016/j.foreco.2022.120487
Received 2 June 2022; Received in revised form 15 August 2022; Accepted 17 August 2022
Available online 5 September 2022

(Karavani et al., 2018, Davis et al., 2018, Falk et al., 2022). The combined impacts of these processes depend on a suite of biotic and abiotic factors at each demographic stage, summarized by a demographic framework (Fig. 1).

Climate warming and changing fire regimes have the potential to impede post-fire tree regeneration by altering these biotic and abiotic factors that govern seedling demography. For example, numerous studies highlight fire effects on availability of viable seeds as a primary mechanism shaping post-fire seedling establishment (e.g., Kemp et al., 2016, Rodman et al., 2020b, Peeler and Smithwick, 2020, Stewart et al., 2021). Seed availability may become more limiting in the future due to shorter intervals between fires and thus time for trees to produce viable seed; through increased fire severity, which leaves fewer surviving seed trees; or through climate-driven reductions in tree fecundity (Enright et al., 2015, Clark et al., 2021, Gill et al., 2022). Vulnerability to these changes varies as a function of species traits. For example, species with serotinous cones can regenerate in the absence of surviving trees, from seeds stored in an aerial seed bank, but the production of serotinous cones is constrained by short fire-return intervals (Buma et al., 2013, Hansen et al., 2018).

Where seeds are available for post-fire germination, variability in fire effects and climate interact to shape the microclimate conditions experienced by seedlings. Post-fire climate conditions have well-recognized effects on tree regeneration (Fig. 1), with relatively cool, moist conditions generally most favorable (e.g., Harvey et al., 2016b, Andrus et al., 2018, Davis et al., 2019a, Rodman et al., 2020b). These regional climate conditions are mediated by local factors, including topography, forest structure and productivity, and understory vegetation (Dobrowski, 2011, De Frenne et al., 2019), which shape local microclimate conditions in post-fire environments (Ma et al., 2010, Carlson et al., 2020b, Crockett and Hurteau, 2022). With climate warming and increased fire activity, reductions in canopy cover and evapotranspiration are expected to result in less microclimatic buffering by vegetation in recently burned areas (Davis et al., 2019b, Wolf et al., 2021), increasing exposure to microclimatic extremes that inhibit regeneration (Carlson et al., 2020a, Hoecker et al., 2020).

Changes in fire severity can also alter microsite factors that influence seedling demography, independent of microclimate. Fires shape the competitive environment and increase the short-term availability of resources such as light, soil nutrients, and seed beds through changes in overstory, understory, and soil conditions (Fig. 1), which can play an important role in providing regeneration opportunities (Johnstone and Chapin, 2006, Parra and Moreno, 2017, Steed and Goeking, 2020). Responses to these varying factors differ among species and are difficult to tease apart, making it challenging to anticipate the impacts of changing fire severity (Urza and Sibold, 2017, Hill and Ex, 2020). For example, high-severity fire results in more stressful, warm-dry microclimate conditions (Wolf et al., 2021), but also a pulse of nutrient availability (Smithwick et al., 2005); sensitivity to these changes will depend on species traits (e.g., drought tolerance). The effects of fires on seed availability, microclimate, and other microsite factors can thus have contrasting effects on seedling demography, complicating our understanding of the influence of fire severity on post-fire tree regeneration.

Among recent work documenting tree regeneration in North America (see reviews by Stevens-Rumann and Morgan, 2019, Coop et al., 2020), post-fire demographic processes have rarely been tracked over time during the first several years after a wildfire, which is often a critical period for setting up long-term vegetation trajectories (e.g., through "priority" effects *sensu* Fukami, 2015; Tepley et al., 2013, 2017, Urza and Sibold, 2017). This leaves a key research gap making it challenging to disentangle the relative importance of biophysical factors at early life stages and how these factors are impacted by changing climate and fire activity.

In this study, we use a demographic filter framework (Davis et al., 2018) to help elucidate mechanisms of forest resilience to two large wildfires in mid-elevation to lower subalpine conifer-dominated forests (hereafter "mixed-conifer" forests) of the northern Rocky Mountains, U.S.A. (Fig. 1). We build on prior research documenting post-fire near-ground atmospheric conditions (Wolf et al., 2021) to quantify the impacts of fire severity on regeneration through its effects on microclimate and other microsite factors, at sites where seed availability was not

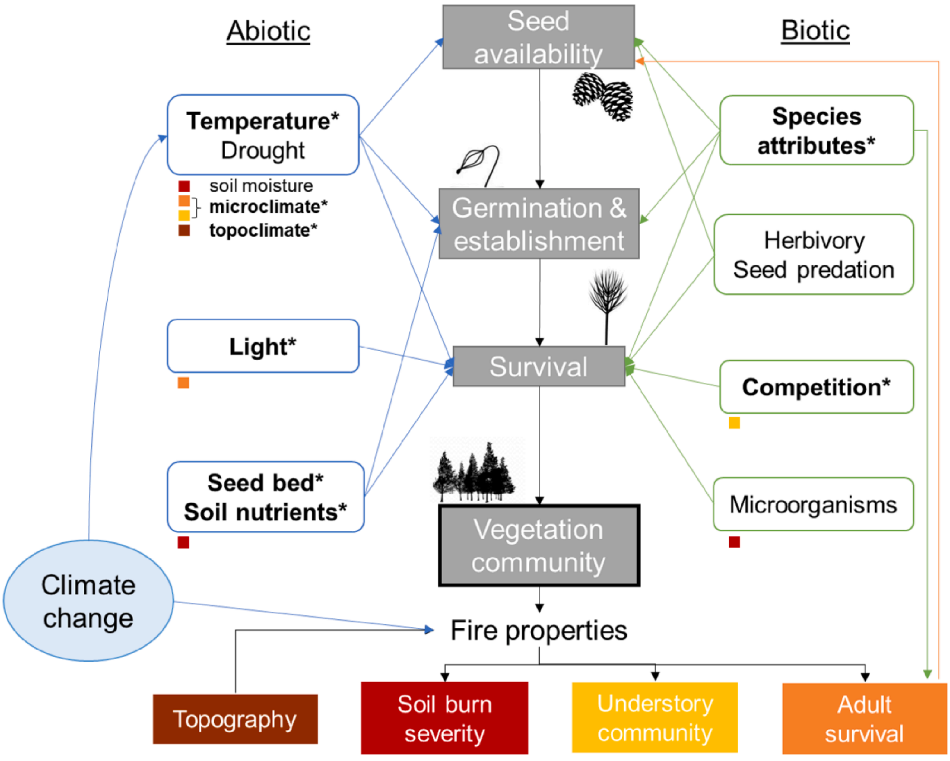

Fig. 1. Demographic filter framework predicting key factors governing post-fire tree regeneration in the context of climate change, adapted from Davis et al. (2018). Conifer regeneration requires passing through three demographic stages (grey rectangles), which are affected by varying abiotic (blue rectangles) and biotic (green rectangles) factors. Fire properties (e.g., intensity, size, spatial patterns) influence these abiotic and biotic conditions in the post-fire environment, and they are in turn influenced by climate (and climate change), the vegetation community, and topography. Factors that are bold with asterisks are accounted for, directly or indirectly, in this study.

limiting. Specifically, we tracked seedlings in two wildfires in western Montana over three years post-fire, and estimated species-specific rates of seedling establishment, survival, and growth in study sites stratified by topographical position and fire severity to capture a range of abiotic and biotic conditions. Our objectives were to: 1) quantify the relative importance of climate, microclimate and fire severity at key seedling demographic stages for dominant conifer species; 2) disentangle the varying impacts of fire severity on seedling demography, including through changes in overstory and understory vegetation composition and structure and soil conditions; and 3) place our findings into the demographic framework to help assess what these examples imply about future forest resilience under climate change. Our results provide a detailed example of contemporary forest response to wildfire, and, more broadly, help to anticipate how ongoing climate warming and changing fire regimes will alter future forest resilience to wildfire.

2. Methods

We characterized post-fire seedling demography by tracking seedling density, survival, and vertical growth in the first three years after fire occurrence to elucidate controls of post-fire tree regeneration. We monitored seedling regeneration in 69 sites across two fires. These include a subset of sites (22 burned and 11 unburned) from a previous study where we monitored microclimate to quantify the impacts of moderate- and high-severity fire on below-canopy atmospheric conditions (Wolf et al., 2021). Our study sites were located using a stratified sampling design to capture a range of biophysical settings (via elevation and aspect) and fire severity (unburned, moderate, high), as described by Wolf et al., (2021).

2.1. Study area

We studied conifer regeneration in mixed-conifer forests within two large wildfires in the Bitterroot Mountains of Montana (Fig. 2). The study area spans forests dominated by ponderosa pine (*Pinus ponderosa*), Douglas-fir (*Pseudotsuga menziesii*), and western larch (*Larix occidentalis*) at low to mid elevations (i.e., <1500 m) and xeric aspects, and lodgepole pine (*Pinus contorta* var. *latifolia*), subalpine fir (*Abies lasiocarpa*), and Engelmann spruce (*Picea engelmannii*) at mid to high elevations (c. 1500–2200 m). Soils are primarily gravelly, well-drained inceptisols derived from volcanic ash overlying metasedimentary, granitic, or mica schist parent material (Soil Survey Staff, 2017). Mean annual temperature at our sites averaged 5.1 °C and total annual precipitation averaged 986 mm from 1981 to 2010, with 22% of precipitation occurring during the growing season of June to September (PRISM Climate Group, 2015).

The Lolo Peak and Sunrise fires burned across c. 22,000 and 11,000 ha, respectively, from July to September 2017, with 15–20% of the burned area classified as high severity (MTBS Project, 2019). Across both fires, > 88% of the area burned was within 100 m of a non-high-severity burn patch, where live trees likely provide seed sources (Fig. A.5). In addition, most of the area in the Lolo Peak (91%) and Sunrise (56%) fires that was more than 100 m from a non-severe patch fell within the elevational range of *Pinus contorta*, which exhibits cone serotiny in this region (personal observation; Harvey et al., 2016b). This spatial patterning of burn severity is consistent with similar wildfires across the northern Rocky Mountains: among a random subset of 30 large fires (>5000 ha) in the region that burned under unusually hot, dry conditions in the regional fire years of 2000, 2003, 2007, 2012, 2015, and 2017, an average of 86% of the area burned was within 100 m of a non-severe patch (Appendix A). Thus, the Lolo Peak and Sunrise fires are representative of other large wildfires in the region that burned during regional fire years with warm, dry summer climate conditions (Morgan et al., 2008).

2.2. Field measurements

We sampled field sites in the first three years after fire (2018–2020) to measure aspects of seeding demography and vegetation change (Table A.1). Seedling density, overstory tree density (defined as trees > 1.37 m height), and live and dead basal area were measured within 60-m-long belt transects that varied from 1 to 10 m in width, with the goal of sampling at least 25–50 seedings per transect while balancing our ability to accurately search the transect area. To minimize uncertainty from age estimates (Hankin et al., 2018), we focused our analyses on total seedling density in the final sampling year in burned sites (i.e., pooling all post-fire seedlings). Post-fire seedlings were easily determined in burned sites, given near-complete surface fire. We restricted seedling counts in unburned sites to post-2017 individuals based on age

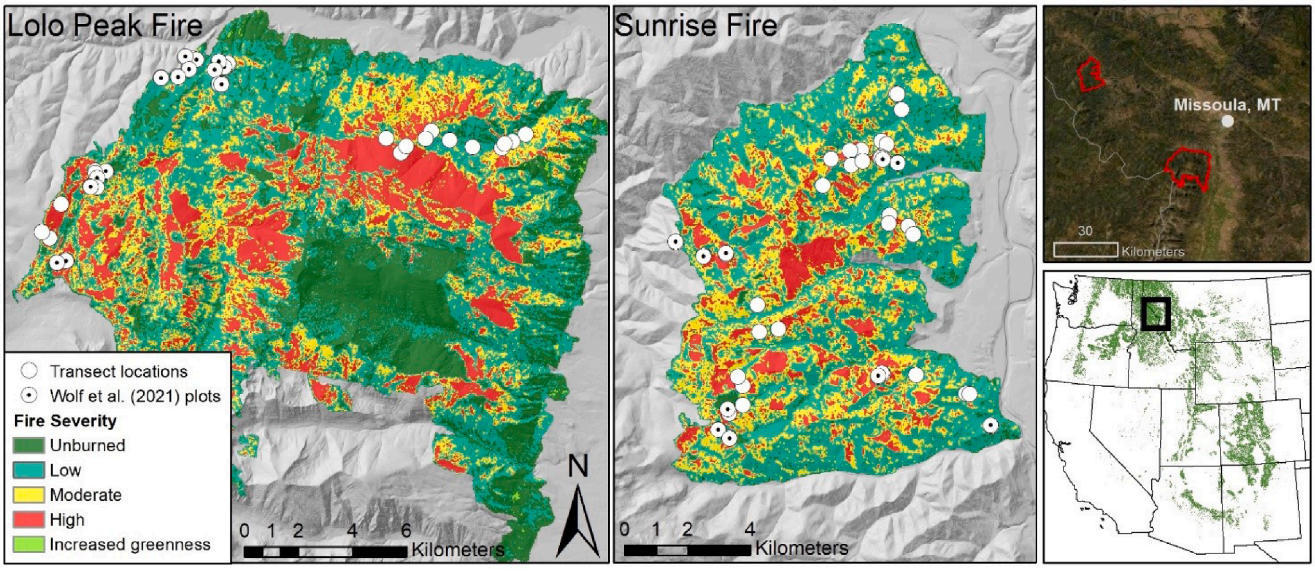

Fig. 2. Map of study area and sample sites in the Lolo Peak (n = 35 sites) and Sunrise fires (n = 34). Sample sites include those that are unique to this study (white circles) and those which also have microclimate measurements published in Wolf et al. (2021) (white circles with black dots). Fire severity classifications are from the Monitoring Trends in Burn Severity project (MTBS Project, 2019), and satellite imagery is from Esri. The green area in the lower right panel delineates the extent of Rocky Mountain forest cover, defined by LANDFIRE's National Vegetation Classification product (landfire.gov).

estimates using height, presence of cotyledons, and bud scars (Urza and Sibold, 2013). We grouped seedlings of *Abies grandis* and *A. lasiocarpa* together in our analyses because *A. grandis* was rare, and distinguishing between germinant seedlings of these species was not always possible. Post-fire planting by USFS overlapped with seven of the 69 sites (10%); planted seedlings were easily distinguishable from natural regeneration based on size and were excluded from analyses.

Within each transect, we established 6–10 permanent 1-m^2 subplots for repeat sampling. Live and dead canopy cover and the distance to the nearest live tree were measured at each subplot, and ocular ground cover measurements were taken to estimate cover of bare ground or rock, litter, coarse woody debris, moss or lichen, forbs, grasses, and shrubs to the nearest five percent. We monitored individual seedlings within 2–10 subplots, with the goal of tracking 10–100 seedlings per site. A total of 1253 seedlings were identified in subplots over the three years, with 212 and 617 in sites that burned at high and moderate severity, respectively, and 424 in unburned sites. We marked seedlings and measured height to track annual survivorship and vertical growth (Table 1).

2.3. Seed source

We used two metrics of potential seed availability: field-measured distance to seed source (*DSS*), and a distance-weighted propagule pressure metric (*PP*) based on post-fire imagery (Table 2). Presence of live trees after fire was identified visually in post-fire imagery in 10 × 10 m grid cells within a 200 m radius circle centered on each site, using post-fire satellite imagery in ESRI basemaps (Environmental Systems Research Institute; 0.5-m resolution) and aerial imagery from NAIP (National Agriculture Imagery Program; 1-m resolution). To account for declining seed dispersal with greater distance from a seed source, live tree cover was distance weighted (i.e., 1 / m from site center) using methods from Coop et al., (2019) to create the PP metric.

2.4. Topoclimate metrics

We used a suite of long-term topoclimate metrics with fine spatial resolution (<1 km) to characterize the biophysical setting of each site (Table 2). Heat load index (*HLI*), calculated at 1/3 arc-second resolution, integrates aspect, slope, and latitude into an index of potential solar heating (McCune and Keon, 2002). Water balance was represented by climatic water deficit (*DEF*, mm), averaged for 1981–2015 from a downscaled (250-m) climate product (Holden et al., 2018). Annual precipitation (ppt_{ann}, mm) and growing-season precipitation (ppt_{JJAS}, mm) were averaged for 1981–2015 from the ClimateWNA product, which interpolates 800-m PRISM grids and adjusts for elevation to generate scale-free climate data (Wang et al., 2016).

2.5. Microclimate metrics

To characterize near-ground microclimate experienced by seedlings, we used field-based measurements from a subset of sites to create a statistical model predicting daily microclimate based on topoclimate, canopy cover, and fire severity variables. The model was based on field measurements at 46 of the 69 sites. To extrapolate beyond these 46 sites, we used linear mixed effects models to predict daily microclimate conditions in all sites over the three study years (Appendix A). Daily predictions were aggregated to the absolute (T_{max}) and the average (T_{avg}) maximum daily temperature over the growing season in each site and year (Table 2).

2.6. Site-level metrics of fire severity

We developed continuous metrics of fire severity at each site, by using a PCA to summarize a suite of field measurements of fire effects, as described by Wolf et al. (2021) and detailed in Appendix A. We interpreted the first two principal components to reflect distinct aspects of fire severity, and use these as predictor variables in statistical models of seedling density (Table 2). PCA Axis 1 (*Axis1*) reflects overstory fire effects, with positive values associated with high tree mortality and char height. PCA Axis 2 (*Axis2*) reflects understory conditions, with positive values associated with greater bare ground cover and negative values associated with greater moss and forb cover.

2.7. Soil inorganic nitrogen

To measure soil inorganic nitrogen content in the first and second year after fire, we collected soil samples at 0, 30, and 60 m along each transect in August-September of 2018 and 2019. To obtain a time-integrated measure of inorganic nitrogen availability, we deployed mesh capsules containing ion-exchange resin (Unibest, Walla Walla, WA, USA), which adsorb ammonium (NH_4^+) and nitrate (NO_3^-) ions in soil solution (Binkley and Matson, 1983). These were placed at c. 5-cm depth in the mineral soil at 0, 30, and 60 m along each transect in August-September 2018, and were allowed to incubate in the field until June 2019 to capture post-thaw N mineralization. See Appendix A for detailed sampling and laboratory analyses.

2.8. Hypothesis testing to evaluate controls of post-fire regeneration

We used statistical models to assess the effects of potential seed sources, microclimate, and fire severity on total seedling density after three years of regeneration, reflecting the net result of germination, establishment, and survivorship (Table 1). We conducted model selection to obtain a best-fit model, and tested the relative influence of controls of regeneration (Fig. A.4). Statistical analyses were conducted in R v. 4.0.4 (R Core Team, 2020).

Seedling counts were modeled separately in burned and unburned

Table 1
Description of the four sets of models used to understand controls of post-fire demographic processes, including the response variables, their scale of measurement, model family, link function, and potential random intercept terms. Sample sizes are reported for regeneration of all species in burned sites. Note that separate models of density, recruitment, and survivorship were built for all species together and for species individually, whereas the growth model included species as a categorical variable.

	Response	Scale of measurement	Sample size	Model family	Link function	Random effects
Density	Net regeneration after 3 yr post-fire	Transect	47 sites	Negative binomial	log	Fire
Recruitment	Annual seedling establishment	Transect	128 site-yr combinations	Negative binomial	log	Fire Site
Survivorship	Inter-annual survival between yr 2 & 3 post-fire	Subplot	186 subplots	Binomial	logit	Fire Site
Growth	Seedling height after 3 yr post-fire	Individual	582 seedlings	Gamma	log	Fire Site Subplot

Table 2
Predictors of seedling regeneration considered in statistical models. Predictors are grouped into broad categories describing key controls of regeneration: potential seed availability, topoclimate/microclimate, and fire effects, each of which includes several subcategories of related variables describing distinct aspects of the three broad controls. Model selection initially included one variable from each subcategory of predictors. Water balance and microclimate variables were not included in the same models because they covaried.

Category	Subcategory	Candidate Variable	Units	Description
Seed availability	Seed source proximity	*PP_dWt*		Propagule pressure, defined as distance-weighted live tree cover in a 200-m radius around site center.
		DSS	m	Plot-averaged distance to the nearest live tree of any species, measured in the field.
		BA_{Spp_L}	$m^2\ ha^{-1}$	Live basal area of focal species, used only in species-specific models.
	Serotiny	BA_{PICO}	$m^2\ ha^{-1}$	Plot-averaged basal area of *P. contorta*, used as a proxy for potential release of serotinous cones. Used only in all-species and PICO models.
	Forest type	$Spp_{present}$	1/0	Binary: 1 if focal species is present in overstory or as a seed source, 0 otherwise. Used only in species-specific models.
(Micro) climate	Topoclimate	*HLI*		Unitless index of potential solar heating.
	Precipitation	*ppt_ann*	mm	35-year average annual precipitation.
		ppt_JJAS	mm	35-year average growing-season precipitation.
		ppt_pf	mm	2-year postfire average growing-season precipitation.
	Water balance vs.	DEF	mm	35-year average climatic water deficit (250 m).
	Microclimate	T_{max}	°C	Modeled post-fire absolute maximum JJAS temperature.
		T_{avg}	°C	Modeled post-fire average daily maximum JJAS temperature.
Fire effects	Overstory	*Axis1*		First principle component of field measurements describing fire severity, with positive values reflecting greater overstory mortality and loss of live canopy cover.
		dnbr		Delta Normalized Burn Ratio: satellite-derived metric of fire severity.
		Canopy	%	Live + dead canopy cover, averaged to site scale for models of seedling density.
	Understory	*Axis2*		Second principle component of field measurements describing fire severity, with positive values reflecting greater bare ground cover and negative values reflecting greater moss and forb cover.
		Cover	%	Six variables describing ground cover in subplots of different vegetation types (Moss, Forb, Grass, Shrub), coarse woody debris (Wood), and bare ground (Bare), which are averaged to site scale for models of seedling density.
	Soil	*soilN*	μg N	Three variables describing resin-capsule inorganic nitrogen (NO_3, NH_4, or total), an integrated measure of
		NO3	day^{-1}	nitrogen availability in years 1–2 post-fire.
		NH4		

sites using negative binomial models with a log link. A model was created for all species combined, and a second set of species-specific models was created for *P. menziesii*, *L. occidentalis*, and *P. contorta* individually. For each model, the random structure was determined by using AICc to compare generalized linear mixed models including a random intercept of fire (i.e., Lolo or Sunrise fire) to generalized linear models with no random effects. We included an offset of log(area) to account for transect size. Fixed-effects predictors were square-root transformed when necessary to reduce skewness, and standardized (z-scores) to facilitate direct comparison among coefficients. We grouped predictors into three broad categories describing fundamental controls of post-fire regeneration: potential seed availability, climate, and fire effects. Each category included subcategories of correlated variables describing distinct aspects of the fundamental controls (Table 2).

To identify an initial set of predictor variables for the statistical models, we first selected one predictor from within each of the eight subcategories of variables; species-specific models included an additional indicator variable for species presence (Table 2). Within each subcategory, we considered the best predictor variable as that with the lowest AICc, and we restricted variables to those with variance inflation factor less than five. The resulting predictors were used for best-fit model selection and hypothesis testing, described below (Fig. A.4).

Using this initial set of predictors, we proceeded with model selection to obtain final, best-fit models for inferring controls of seedling density. We dropped terms that did not significantly improve fit (ΔAICc < 2), and added quadratic terms and two-way interaction terms describing plausible ecological relationships if they improved fit. Model skill was evaluated using AICc, marginal pseudo-R^2 values (Bartoń, 2022), and raw (ρ) and cross-validated (ρ-CV) Spearman correlations between observed and predicted values (details in Appendix A). We conducted k-fold cross-validation by holding out 25% of the data for validation, training the model on the remaining data, and averaging ρ over 1000 repetitions. We assessed residuals visually and used semi-variograms to evaluate spatial autocorrelation. Partial effects and 95% confidence intervals were calculated using the *effects* package (Fox and Weisberg, 2018).

To explicitly test the relative influence of the varying controls of post-fire regeneration predicted by a demographic framework (Fig. 1), we used the initial set of variables to compare models containing subsets of predictors describing seed sources, climate, and fire severity (Table B.1). Each subset model was compared with the next-simplest model using log-likelihood ratio tests to assess the added explanatory power of sets of variables in each category. To evaluate different climate metrics, we compared models including microclimate variables in place of climatic water deficit (*DEF*, Table 2); microclimate and *DEF* were not included in the same models because they were well-correlated ($r = 0.61$, $p < 0.001$; $t = 6.3$, $df = 69$).

2.9. Seedling demographic stages: Annual recruitment, survivorship, & growth

We utilized annual seedling recruitment, survivorship, and height data to assess the influence of biotic and abiotic factors at each demographic stage (Table 1). To evaluate temporal as well as spatial variability in regeneration, we built statistical models of annual recruitment in burned sites, defined as the density of germination-year seedlings alive in August-September of each sampling year at each site. We avoided problems of aging uncertainty by restricting this analysis to germination-year seedlings (identified based on the presence of cotyledons). Recruitment was modeled using the same methods as for

seedling density to obtain a best-fit model. We included a random intercept of site to account for repeated measurements, and predictor variables included those in Table 2 and post-fire year.

To evaluate the influence of microclimate and microsite factors on seedling survivorship, we used binomial mixed effects models with a logit link. To account for lack of independence among observations from repeat sampling, and among observations from subplots within the same site, we restricted our analysis to year three after fire and included a random effect of site. The binomial response variable was the count of marked seedlings in each subplot that survived or died between the 2019 and 2020 measurements (Table 1). Fixed-effects predictors included seedling age and those described in Table 2 under the broad categories of climate and fire effects. We used annual subplot-specific (i.e., not site-averaged) measurements of canopy and ground cover as predictors, to assess the influence of microsite conditions on survivorship. We calculated area under the receiver operating curves (AUC) using the *pROC* package (Robin et al., 2011; see Appendix A). Simulation-based tests of residuals from the *DHARMa* package (Hartig, 2021) were used to assess dispersion.

To evaluate the effects of species, age, and site characteristics on growth, we built a generalized linear mixed-effects model of seedling height. We restricted our analysis to data from year three after fire and used random effects of subplot nested within site to conform to assumptions of independence. A gamma distribution with a log link was used to account for greater variance in height among taller seedlings. Predictors included species, seedling age, and climate variables and fire-effects variables described in Table 2.

3. Results

Regeneration was abundant by the third year after fire, with a median density among all sites of 2,633 seedlings per hectare (IQR 750 to 7500 ha^{-1}). All burned sites (n = 47) had at least one live seedling, four sites (8.5%) had densities < 100 ha^{-1}, and 12 sites (26%) had densities > 10,000 ha^{-1}. Seedling density was significantly greater in burned than unburned sites on average for *P. contorta*, *P. ponderosa*, and *L. occidentalis* (Fig. 3). Comparing post-fire seedling densities with reconstructed pre-fire tree densities, two-thirds of burned sites were at or above replacement density three years post-fire, and species composition of seedlings generally reflected pre-fire composition of mature trees (Fig. B.1, B.2). The most common species pre- and post-fire were *P. menziesii* and *P. contorta*, present in > 50% of sites.

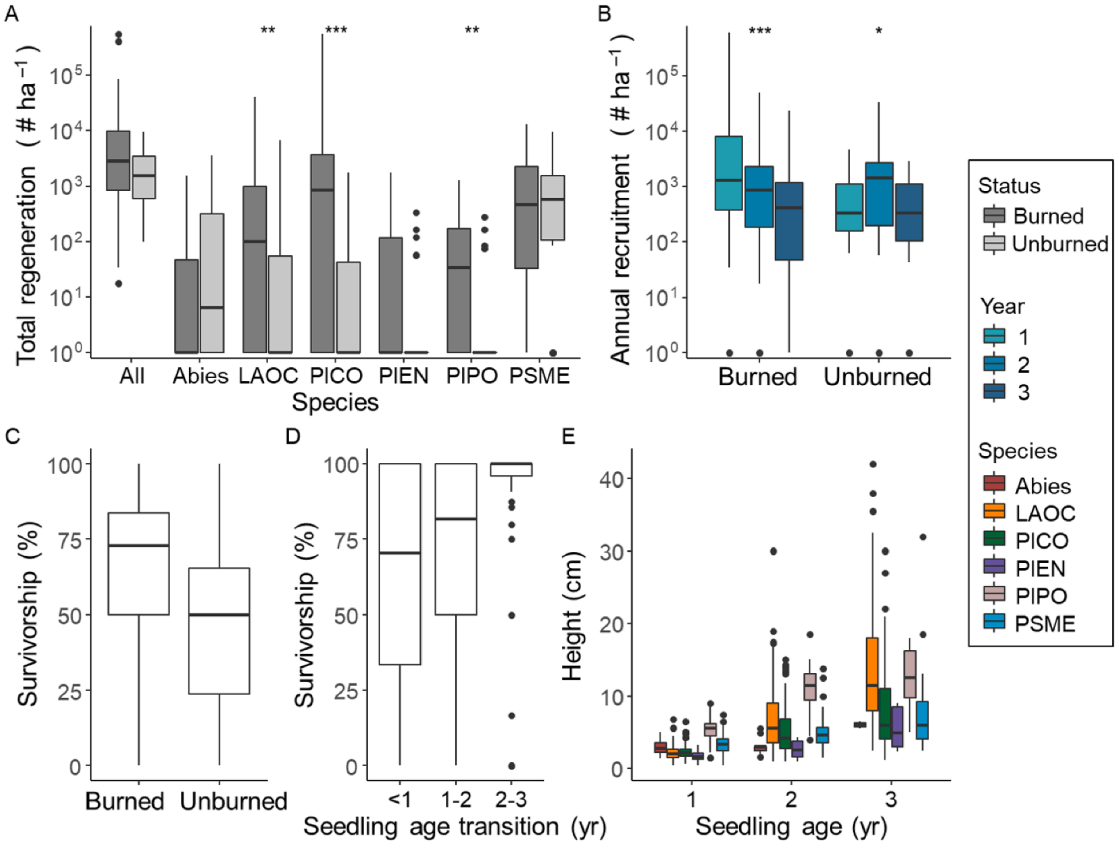

Fig. 3. Estimates of total regeneration, annual recruitment, seedling survivorship, and height measurements over the first three years after fire. ***A:*** Total regeneration of all species and individual species in burned and unburned sites. ***B:*** Annual recruitment (density of germination-year seedlings) in burned and unburned sites. A constant of 1 was added to seedling density values to allow them to be represented on a log scale. Asterisks indicate statistical significance of nonparametric Wilcoxon rank-sum tests comparing burned and unburned sites (A), and Friedman tests comparing years (B) [* $p < 0.05$, ** $p < 0.01$, *** $p < 0.001$]. ***C:*** Total percent survivorship of all marked seedlings over 2018–2020 in burned and unburned sites. ***D:*** Annual survivorship of marked seedlings across different age transitions: < 1 yr is intra-annual survival of germination-year seedlings; 1–2 is inter-annual survival from the first to the second growing season of life; and 2–3 is inter-annual survival from the second to the third growing season. Survivorship values for each age transition differ in the sampling window over which they were measured, and not all age-sampling year combinations are represented in the dataset; intra-annual survivorship of germinant seedlings was only measured once, from June to August/September 2019. ***E:*** Seedling height measurements grouped by age and species. Boxes enclose the central 50% of data, dark horizontal lines indicate medians, and upper and lower vertical lines extend to the largest/smallest observation that is less than or equal to 1.5 times the interquartile range outside of the box; dots indicate outliers.

3.1. Relative influence of potential seed availability, climate, and fire severity on seedling densities

The best-fit model for total seedling density in burned sites accounted for c. 75% of the variability among sites (marginal pseudo-R^2), and had a high cross-validated correlation between predicted and observed values (ρ-CV = 0.63). Seedling density was negatively related with distance to seed source, negatively related with T_{max}, representing microclimate, and varied with *Axis1*, *Axis2*, and *soilN*, reflecting distinct aspects of fire severity (Fig. B.3). Total seedling density increased with overstory fire severity (*Axis1*) and moss and forb cover (*Axis2*), and decreased with greater soil nitrogen availability (*soilN*). These general patterns were largely consistent among species, although the specific variables retained and their relative influence differed (Fig. 4; Table B.2). In particular, the effects of fire severity metrics were not uniform, indicating that the influence of microsite conditions on regeneration varied among species. Notably, *P. menziesii* seedling density had a negative relationship with fire severity and no relationship with soil nitrogen variables, in contrast to overall trends with species combined, while *P. contorta* density was positively related with coarse wood cover (Fig. 4). Some relationships of seedling density with microsite variables also differed between burned and unburned sites (Fig. B.3, B.4).

Variables describing seed source proximity or density explained 50% of the total variability in seedling densities among sites (Table B.1). Total density was greater at sites closer to live seed sources and with a greater abundance of pre-fire *P. contorta* (BA_{PICO}), representing a proxy for seeds from serotinous cones. *P. contorta* also had the highest median (25,270 ha^{-1}) and maximum (>500,000 ha^{-1}) post-fire seedling density among all species. After accounting for potential seed availability, the addition of variables describing topoclimate improved model fit, resulting in an increase in the marginal pseudo-R^2 from 50% ("Seed" model) to 62% ("Seed + Clim" model; Fig. 4, Table B.1). The further addition of microclimate information slightly improved model fit ("Seed + MC" model, Fig. 4; marginal pseudo-R^2 = 64%), indicating that the influence of spatial climate variability on seedling density was largely captured by topoclimate metrics. Finally, after accounting for potential seed availability and microclimate, variables describing fire severity substantially improved model fit ("Seed + MC + Fire" model, Fig. 4; marginal pseudo-R^2 = 78%).

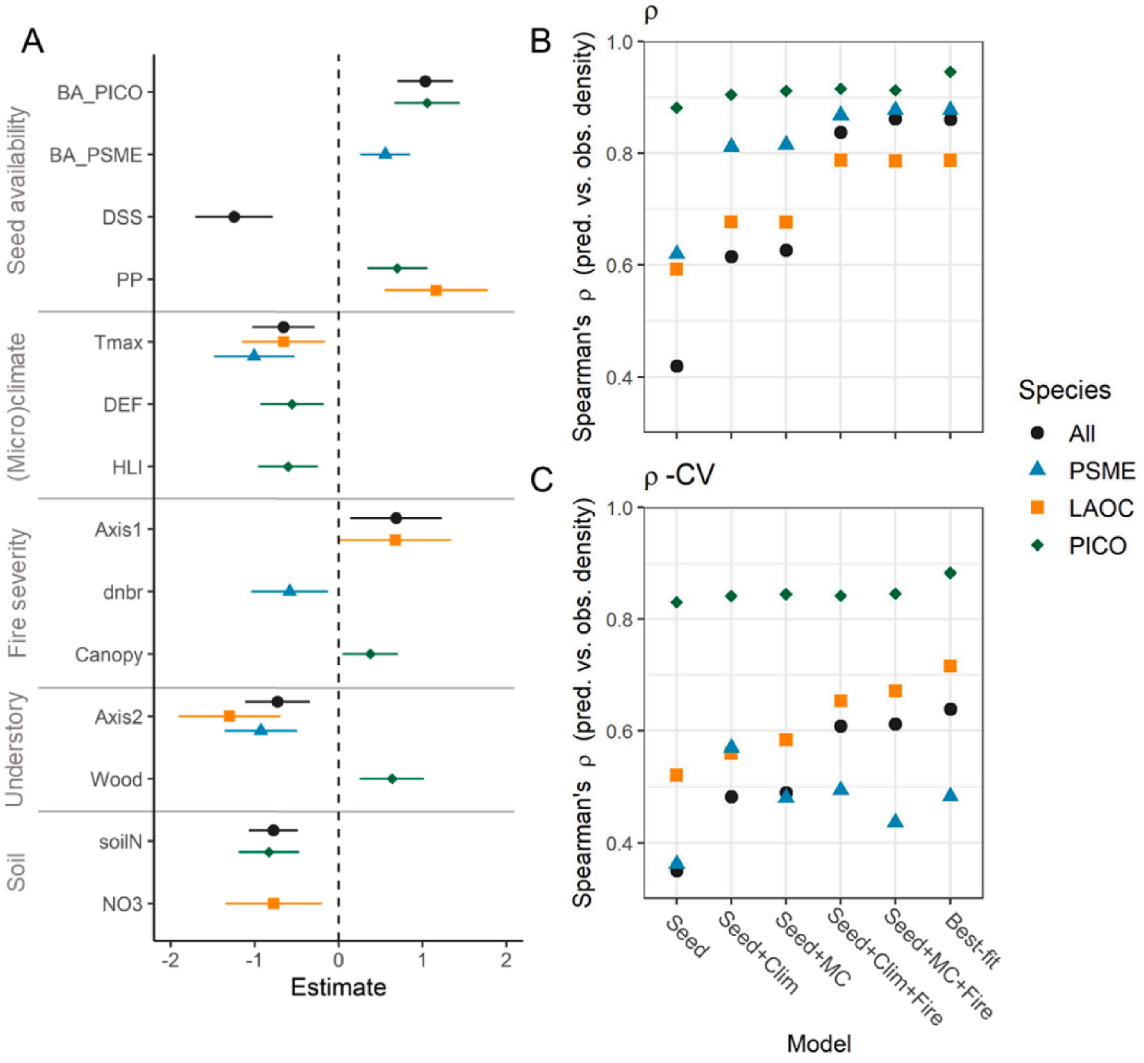

Fig. 4. Best-fit models of seedling density in year three after fire in burned sites, and the relative influence of (micro)climate and fire severity on regeneration after accounting for factors that influence seed availability. Results are presented for models of total (all-species) seedling density and for individual species: *P. menziesii* (PSME), *L. occidentalis* (LAOC), *P. contorta* (PICO). Predictors are grouped into categories describing potential seed availability ("Seed"), fire effects ("Fire"), and microclimate ("MC") or topoclimate ("Clim"), described in Table 2. ***A:*** Estimates of main effects and 95% confidence intervals for best-fit models. ***B, C:*** Comparison of models including subsets of predictors, showing correlations between observed and predicted values (B) and cross-validation results (C).

3.2. Seedling demographic stages: Annual recruitment, survivorship, & vertical growth

Annual recruitment in burned sites varied among species and declined over time, with greater recruitment in the first year (median 1292 ha^{-1}) compared to the second (850 ha^{-1}) and third (417 ha^{-1}) year post-fire (Fig. 3). Annual recruitment was largely influenced by the same variables that influenced total seedling density, but with added nuance from an interaction between post-fire year and basal area of *P. contorta*, and interactions involving HLI, precipitation, and forb cover (Table B.3, Fig. 5).

Seedling survival was high, with a median of 66% (IQR 46 – 82%) cumulative survivorship of all seedlings tracked during the study period. Overall survivorship was higher on average in burned sites (median 73%, IQR 50–84%) compared to unburned sites (median 50%, IQR 24–65%; Fig. 3). Among sites in which survivorship could be estimated for each species, overall survival was highest (>80%) for *P. contorta* (22 sites), *L. occidentalis* (14 sites), and *Abies* spp. (4 sites), with lower survival (averaging 50%) survival for *P. menziesii* (31 sites), *P. ponderosa* (7 sites), and *P. engelmannii* (5 sites). At annual timescales, survivorship varied with seedling age, with the lowest survival within the germination year (Fig. 3). In burned sites, annual seedling survivorship between the second and third year after fire was positively related to seedling age, canopy cover (*Canopy*, subplot scale), and total moss and forb cover (*Moss & Forb*, subplot scale), and negatively related to *DEF* and resin nitrate (*NO3*), with a model AUC of 0.77 (Fig. 6). Expected probability of survival decreased with higher *DEF*, but only for seedlings of younger ages (Fig. 6A).

Seedling height after three years was positively related to microclimate (T_{avg}) and moss and forb cover (*Axis2*), with the most pronounced growth in sites with warm, dry microclimate (Fig. B.5). Seedling height also varied among species ($p < 0.001$, Kruskal-Wallis $X^2 = 43.2$, df = 5). *P. engelmannii* seedlings were the smallest on average after three years, while *L. occidentalis* and *P. ponderosa* were the largest on average (Fig. 3). *L. occidentalis* grew fastest over the three-year period, with median height of 11.5 cm (IQR 8–18 cm) at age three and a maximum of 42 cm.

4. Discussion

Our findings of abundant tree regeneration provide an important example of how forests can exhibit early resilience to contemporary fire activity, even in the context of increasingly stressful climate conditions for post-fire tree regeneration over the 21st century (e.g., Davis et al., 2019a). Biophysical aspects of the pre- and post-fire environments helped explain over 75% of the variability observed in post-fire conifer density in the two large fires we studied, supporting predictions based on the demographic framework used to frame our study (Fig. 1). This understanding elucidates the relative importance of fire effects on microclimate and microsite factors that influence recruitment, survival, and growth, and helps anticipate how forest resilience to wildfires may change under changing climate.

4.1. Evidence of forest resilience to wildfire

Mixed-conifer forests at our sites exhibited signs of resilience to recent moderate- and high-severity wildfire. Given abundant natural post-fire regeneration (Fig. 3, Fig. B.1), we expect these sites to develop species composition and stand characteristics broadly similar to pre-fire conditions. The regeneration observed in these individual fires contrasts with recent observations of declines in post-fire conifer regeneration at larger regional scales in the northern Rocky Mountains and across the West (Donato et al., 2016, Stevens-Rumann et al., 2018, Davis et al., 2019a, Rodman et al., 2020a). We attribute this robust regeneration in part to moderate post-fire climate conditions experienced from 2018 to 2020, which supported high rates of seedling survival (Fig. 3). Growing-

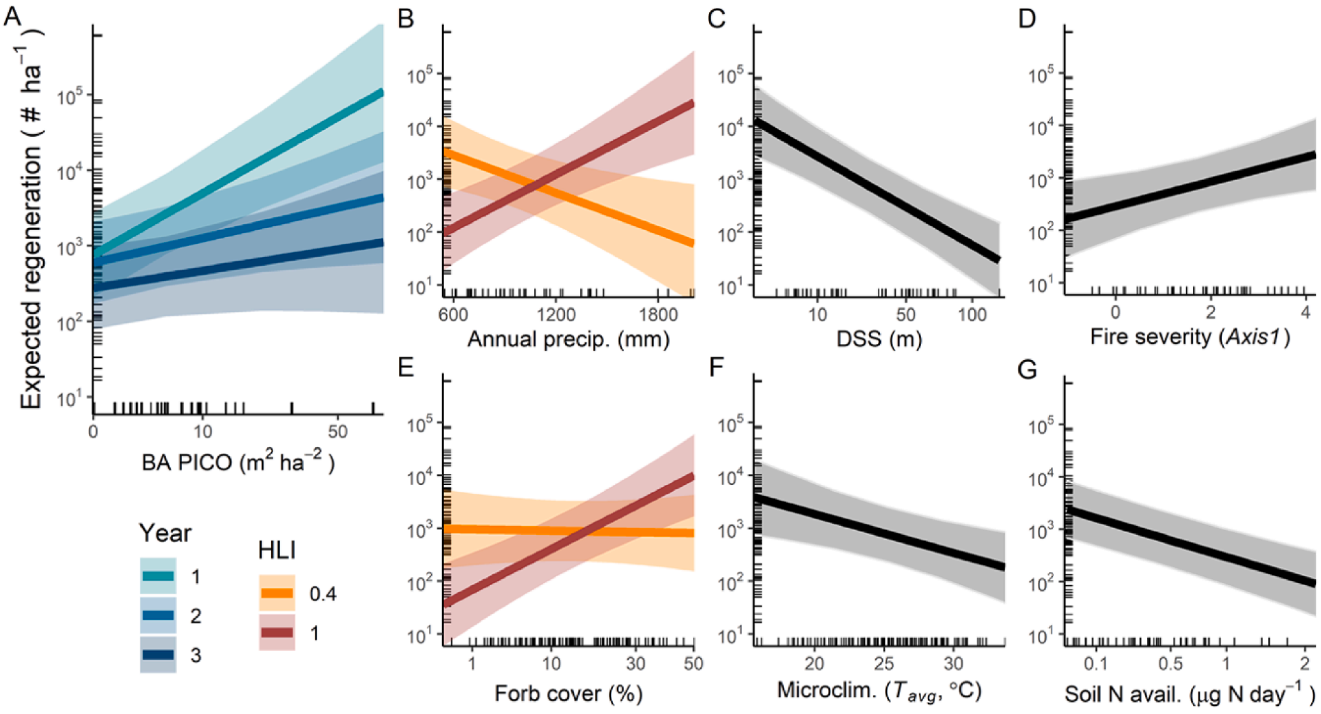

Fig. 5. Partial effects plots for best-fit model of annual seedling recruitment in burned sites (all species), with 95% confidence intervals. Legend text: "Year" is years since fire; "HLI" is heat load index. Variables include (A) total basal area of *P. contorta* ("BA PICO"); (B) 30-yr average total annual precipitation; (C) distance to potential seed source ("DSS"); (D) fire severity, as represented by PCA Axis 1 scores (see methods); (E) forb cover (annual); (F) microclimate, represented by average daily summer temperature (annual); and (G) soil nitrogen availability. Note that x-axis scales are back-transformed from z-scores used in model fitting to represent predictor variables in their native units, and x-axis scales in panels A, C, E, and G also reflect a square-root transformation. Ticks on the x- and y-axes represent the observed values.

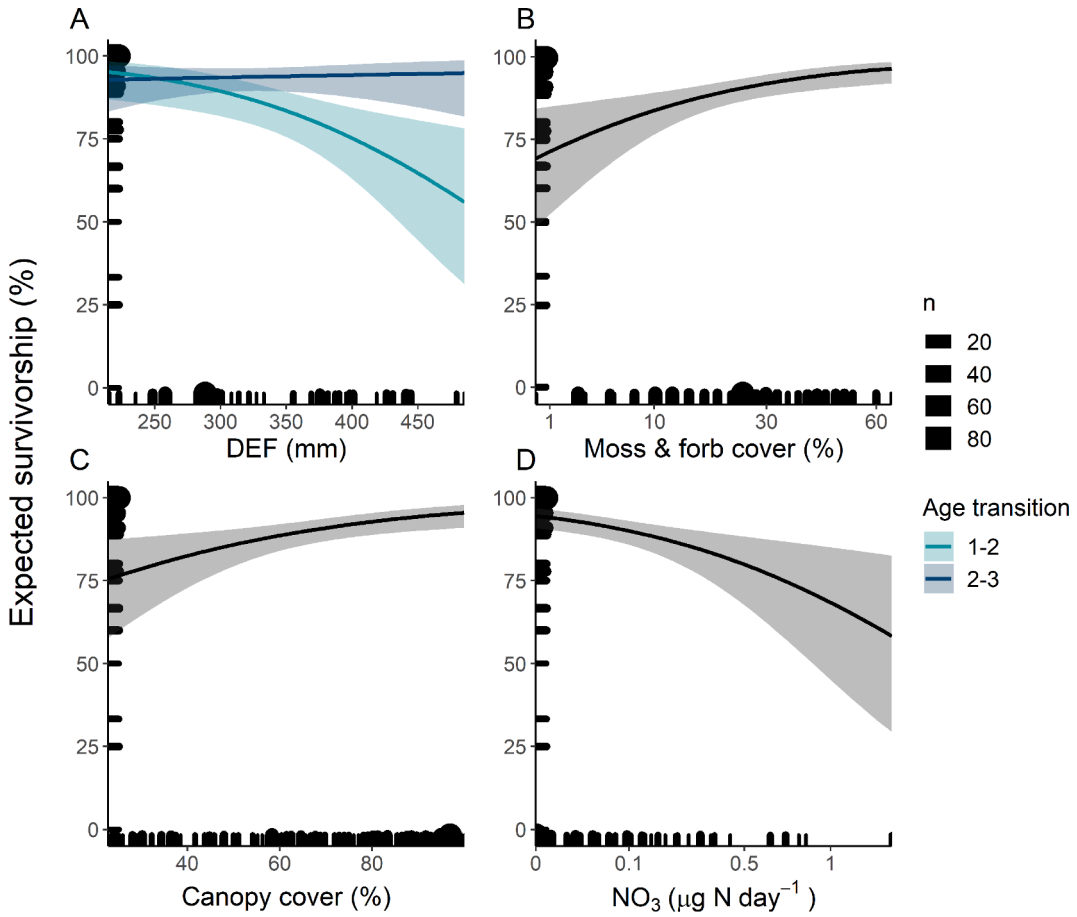

Fig. 6. Partial effects plots for best-fit model of seedling survivorship (all species) between post-fire years two and three in subplots within burned sites, with 95% confidence intervals. Marker sizes on axes indicate the number of seedlings (n) represented by the survivorship estimate in each subplot (Table 1); only subplots with marked seedlings alive in post-fire year two are included. Seedling age transitions are given in years: 1–2 is inter-annual survival from the first to the second growing season of life; 2–3 is inter-annual survival from the second to the third growing season of life. Variables include (A) 30-yr average climatic water deficit ("DEF"); (B) average of moss and forb cover at each subplot; (C) total canopy cover at each subplot; (D) nitrate (NO_3) availability estimated using resin capsules (Table 2). Note that x-axis scales are back-transformed from z-scores used in model fitting to represent predictor variables in their native units, and x-axis scales in panels B and D also reflect a square-root transformation.

season (June-September) daily maximum temperatures in 2018–2020 averaged only 0.3 °C (0.21 sd) above the 1981–2020 mean in Missoula, Montana, with precipitation only 32 mm (0.63 sd) below average (Western Regional Climate Center, 2021); these values varied little among the three study years (Fig. A.1). Similarly, recent studies in the eastern Cascade Mountains of Washington provide examples of robust conifer regeneration under mild post-fire climate conditions (Littlefield 2019, Povak et al., 2020).

Importantly, all of our sites were within 100 m of a live seed source, by design, so our findings apply to locations where dispersal distance is not severely limiting to seed availability (e.g., Kemp et al., 2016, Chambers et al., 2016, Littlefield, 2019, Peeler and Smithwick, 2020). Although we did not sample across a full range of distance-to-seed-source values, the fires studied here are characterized by complex spatial patterns of fire severity, as is common within even large fires in the region (e.g., Turner et al., 1994, Harvey et al., 2016a). As such, our sites are representative of the majority of burned areas within these fires, which are proximate to potential seed sources (Fig. A.5).

A key uncertainty in our ability to anticipate forest resilience to these wildfires is whether the initial patterns of regeneration observed here will be maintained, to ultimately determine longer-term trajectories in tree densities and species composition (Gill et al., 2017). Given the context of directional climate warming, it is possible that the observed early resilience could be undermined by future tree mortality events. For example, *P. ponderosa* seedlings in northern Arizona experienced substantial mortality (65%) due to drought conditions five years after cohort initiation (Kolb et al., 2020). Nevertheless, our finding of increasing survival with seedling age (Fig. 3) suggests that only a severe drought or subsequent disturbance would alter the successional trajectories established thus far. While the long-term fate of these forests is unknown, our findings exemplify mechanisms of post-fire forest recovery that are likely operating within the "safe operating space" defined by the historical range of variability (Johnstone et al., 2016).

4.2. *Mechanisms of forest resilience to wildfires*

We identify three key mechanisms of resilience to moderate- and high-severity wildfires in these mixed-conifer forests. First, the availability of viable seeds consistently serves as the first biotic filter to overcome for post-fire tree regeneration (Davis et al., 2018, Stevens-Rumann and Morgan, 2019) (Figs. 4-5). While we used distance to seed source as a coarse metric for seed rain, its importance in our statistical models highlights the need to account for potential seed availability when evaluating the influence of other factors on post-fire regeneration (e.g., fire severity). Secondly, our results demonstrate how post-fire regeneration depends on microclimate conditions, reflecting an interaction between climate and fire severity. Finally, our results underscore that fire itself facilitates tree regeneration, with heterogeneity in fire effects at multiple scales supporting regeneration via seed provision and microsite diversity. Our results are consistent with

demographic predictions and observational studies from conifer forests across the West highlighting seed dispersal and climate as key filters on post-fire regeneration (e.g., Harvey et al., 2016b, Stevens-Rumann et al., 2018, Kemp et al., 2019, Rodman et al., 2020b, Busby and Holz, 2022; Fig. 1). Further, this study provides an example revealing how microsite factors affected by fire severity can either facilitate or limit regeneration.

Our findings highlight important influences of post-fire microclimate conditions on seedling establishment and survival. Total seedling densities, annual recruitment, and annual survivorship were all higher in relatively cool-wet sites (Figs. 4-6), indicating that regeneration was sensitive to near-ground microclimate conditions. The impacts of microclimate on regeneration are strongest in early life stages, when juveniles are vulnerable to desiccation or heat-induced mortality from warm, dry atmospheric or soil conditions (Kolb and Robberecht, 1996, Johnson et al., 2011, Miller and Johnson, 2017). We found that seedling survival was most sensitive to climate between the germination year and the second year of life (Fig. 6A), supporting the idea that weather and climate conditions during the germination year serve as an important mortality filter affecting forest regeneration (Stein and Kimberling, 2003).

Our results further demonstrate how fire plays a vital role in facilitating regeneration in these forests. Seedling recruitment was strongly predicted by the basal area of *P. contorta* in the first year after fire, demonstrating the likely importance of serotiny in driving initial post-fire regeneration where *P. contorta* was present (Fig. 5A). Further, initial recruitment and survival were greater on average in burned sites compared to unburned sites, implying more favorable site conditions for seedlings after fire (Fig. 3). Moderate- and high-severity wildfire increase the availability of resources such as light, favorable seed beds, and growth-limiting nutrients (e.g., Pausas et al., 2002, Urza and Sibold, 2017), which limit regeneration in unburned forest (Fig. B.4, B.6). Declining recruitment by the third year after fire implies that such favorable conditions are short-lived, with initial patterns of establishment during this "window of opportunity" ultimately shaping forest trajectories (Karavani et al., 2018).

The contrasting impacts of recent wildfire on regeneration – through both increased resource availability and exposure to microclimatic extremes – illustrates how high-severity fire creates trade-offs that govern post-fire conifer seedling demography. For example, seedling recruitment was higher in sites with greater tree mortality given similar distance to seed source (Fig. 5D). This implies that while some remaining canopy cover, even dead, supports regeneration through microclimatic buffering, overstory mortality also supports regeneration, via greater light availability and/or increased soil moisture due to reduced canopy interception and evapotranspiration (Ma et al., 2010, Parra and Moreno, 2017, Rodman et al., 2020b, Kolb et al., 2020). Responses to this trade-off varied among species; for instance, *P. menziesii* seedling density was greater in sites that burned at lower severity (Fig. 4A), indicating greater germination and survival in cooler, more shaded environments. This pattern is consistent with prior studies and the greater shade-tolerance of *P. menziesii* compared to *P. contorta*, *L. occidentalis*, or *P. ponderosa* (Minore, 1979, Rodman et al., 2020b).

Fire severity thus alters biophysical factors in ways that both promote and impede the regeneration of each conifer species. Our findings imply that soil nitrogen availability represents another such trade-off. Consistent with a widely-observed short-term N pulse after fire (Smithwick et al., 2005), nitrogen availability was elevated in burned soils (Fig. B.6). High post-fire soil inorganic nitrogen was associated with low seedling recruitment and survival (Fig. 5G, 6D), with the exception of *P. menziesii*. High N supply could stimulate aboveground growth without commensurate root development, potentially inhibiting seedling drought resistance and survival (Isaac and Hopkins, 1937, Bensend, 1943, Nilsen, 1995). Alternatively, elevated soil inorganic nitrogen may be associated with other changes, such as reduced mycorrhizal abundance and diversity (Taudière et al., 2017, Remke et al., 2020) or enhanced erosion (Certini, 2005). Additional research is needed to evaluate how fire effects on soil physical properties, biogeochemical processes, and biota affect seedling physiology and demography. Nevertheless, our results imply that while some N availability and exposure of mineral seed beds may generally benefit seedlings (Fig. B.4), severe soil impacts likely inhibit regeneration.

These multifaceted effects of fire severity highlight how burn mosaics can promote forest resilience. At patch scales (e.g., 10^2 –10^4 m^2; Coop et al., 2019), heterogeneity in tree mortality provides seed sources, while at finer microsite scales, heterogeneous canopy and understory environments facilitate regeneration. For example, *P. menziesii* and *L. occidentalis* seedling densities (Fig. 4) and all-species density, survival, and growth (Fig. 6, Fig. B.5) were higher in sites with greater moss and forb cover and less bare ground cover. Moss and forb cover could serve as a proxy for greater surface soil moisture or less competition from shrubs and grasses (Wagner et al., 1989, Landhausser et al., 1996, Plamboeck et al., 2008, Kolb et al., 2020, Carlson et al., 2020a). Indeed, forb cover (mostly *Chamaenerion angustifolium*) had a larger positive effect on recruitment on south- than north-facing sites (Fig. 5E), suggesting a potential facilitative effect through microclimatic buffering. This finding is consistent with studies demonstrating how shrubs can facilitate seedling establishment in semiarid environments (Urza et al., 2019, Crockett and Hurteau, 2022), and it highlights the possibility that forbs could play a similar role as nurse plants in more mesic sites in the northern Rocky Mountains. Conversely, extensive bare soil may be associated with high surface temperatures or vulnerability to erosion (Certini, 2005). While sites burned at higher severity had more bare ground and less forb cover ($\rho = 0.67$ and $\rho = -0.47$, respectively; $p < 0.001$, $n = 47$), moss and coarse wood cover did not differ with fire severity, suggesting that high-severity patches can harbor favorable below-canopy microsites. Thus, fine-scale heterogeneity in fire effects promotes resilience even within areas of stand-replacing fire.

Several limitations to this study highlight priorities for continued research. Most critically, the regeneration patterns observed here could be altered by continued recruitment or mortality (Gill et al., 2017, Kolb et al., 2020). Future research should quantify changes in climate sensitivity as seedlings age, to evaluate vulnerability to climatic extremes over time. Additional research priorities include investigating what drives differing sensitivity among species, for example the contrasting responses to soil nitrogen availability and overstory fire severity in *P. menziesii* compared with general trends (Fig. 4, Table B.4). In addition, our study did not consider post-fire contingencies of seed masting in conifers; *P. ponderosa* recruitment was low in our sites relative to co-occurring species, and it is unclear if this is due to environmental drivers or a lack of mast years during the sampling window (Keyes et al., 2015). Regeneration was likely also influenced by unmeasured factors, including soil moisture, seed predation, and herbivory (Fig. 1). Although our interpretations are limited to a narrow range of conditions, our findings demonstrate the utility of a demographic framework for predicting the dominant controls of post-fire conifer regeneration.

4.3. Implications for forest management

Our findings support three important management approaches used to promote or maintain forest resilience to wildfires. First, a diversity of microsite conditions supported regeneration, implying that heterogeneity in pre-fire forest structure, fire severity, and post-fire understory communities can create microrefugia for tree seedlings. Our results thus support the use of fuel treatments in low- and mixed-severity fire regimes, under the goal of promoting patch and microsite diversity (Prichard et al., 2021). While fuels management is less effective in subalpine forests with high-severity fire regimes (Halofsky et al., 2018), allowing fires to burn under moderate fire weather could achieve similar goals by promoting heterogeneity in fire effects.

Second, our results bolster the understanding that post-fire planting is most effective in areas lacking seed sources and in relatively cool-wet topographical settings, with residual structures to provide shading, and

with little competition from shrubs and grasses (e.g., Stevens-Rumann and Morgan 2019) (Figs. 5-6). Finally, our results support the utility of predictive spatial models for reforestation planning (Holden et al., 2021). Despite the importance of field-based microclimate metrics, our statistical models also did an excellent job explaining seedling density based on topoclimate and fire severity alone (Fig. 4, Table B.1), suggesting that fine-scale (250-m) climate data capture spatial variation in microclimate that is useful in management contexts.

4.4. Anticipating forest resilience under changing climate and fire regimes

Climate change over the remainder of the 21st century has the potential to undermine the forest resilience observed in this study, directly via more stressful climate conditions, indirectly via higher fire activity, and through interactions between climate and fire that alter local microclimate conditions (Fig. 5F). Our results imply that fire-caused canopy loss can amplify the impacts of climate warming on regeneration by increasing exposure to warm-dry extremes (Zellweger et al., 2020), particularly in the first few years after fire prior to vegetation recovery, and in relatively cool-wet forests where canopy loss has a larger absolute effect on microclimate (Davis et al., 2019b, Wolf et al., 2021). Indeed, other studies from the Rocky Mountains highlight the potential for short-interval severe fire to sharply curtail regeneration via seed limitation and stressful post-fire microclimate and soil conditions (e.g., Turner et al., 2019, Hoecker et al., 2020, Rammer et al., 2021). Forest development will thus depend on microclimate conditions and the frequency, severity, and spatial patterning of fire.

Finally, varied responses to fire severity among species (Fig. 4A) suggest that fire-relevant traits will govern post-fire seedling demography, ultimately driving changes in species composition anticipated under climate change. For example, our finding of greater *P. menziesii* recruitment in sites with remaining canopy cover (Fig. 4, Table B.3) suggests that it may be particularly vulnerable to increased fire severity. In contrast, we found that *L. occidentalis* was fast-growing (Fig. B.5) and regenerated at greater densities in areas of high overstory fire severity (Fig. 4), implying that it may be well-suited to take advantage of high-light, recently disturbed areas (Steed and Goeking, 2020). In contrast to regeneration failures expected at lower-treeline ecotones where warming exceeds species tolerances (Davis et al., 2019a), wildfires in mid- and high-elevation forests have the potential to catalyze shifts in relative abundances in areas of overlapping species distributions (Hoecker and Turner, 2022).

CRediT authorship contribution statement

Kyra Clark-Wolf: Conceptualization, Methodology, Formal analysis, Investigation, Visualization, Funding acquisition, Writing - original draft. **Philip E. Higuera:** Conceptualization, Methodology, Resources, Supervision, Funding acquisition, Writing - review & editing. **Kimberley T. Davis:** Conceptualization, Methodology, Resources, Funding acquisition, Writing - review & editing.

Declaration of Competing Interest

The authors declare that they have no known competing financial interests or personal relationships that could have appeared to influence the work reported in this paper.

Acknowledgements

We thank undergraduate assistants A. Hendryx, M. Miller, R. Kirk-Davidoff, D. Darter, and S. Ammentorp for their help with data collection and entry. We thank Z. Holden for sharing climate data, A. Shaw and C. Cleveland for methodological instruction, and V. Archer for support for the project and insights on the study region. We are grateful to Kurt Wetzstein and the Lolo National Forest for cooperation with site selection and sampling. We thank S. Dobrowski for contributions to our study of post-fire microclimate. This work was supported by grants from the Joint Fire Science Program, through Graduate Research Innovation program award 18-1-01-53 (to KCW, PEH, KTD), and award 16-1-01-15 (to KTD and PEH).

Open research statement

Data and code are publicly available via Dryad: https://doi.org/10.5061/dryad.9s4mw6mhj.

Appendix A. Supplementary data

Supplementary data to this article can be found online at https://doi.org/10.1016/j.foreco.2022.120487.

References

Abatzoglou, J.T., Williams, A.P., 2016. Impact of anthropogenic climate change on wildfire across western US forests. Proc. Natl. Acad. Sci. 113, 11770–11775.
Andrus, R.A., Harvey, B.J., Rodman, K.C., Hart, S.J., Veblen, T.T., 2018. Moisture availability limits subalpine tree establishment. Ecology 99, 567–575.
Bartoń, K., 2022. February 24. Multi-Model Inference, MuMIn.
Bensend, D. W. 1943. Effect of Nitrogen on Growth and Drouth Resistance of Jack Pine Seedlings.
Binkley, D., Matson, P., 1983. Ion Exchange Resin Bag Method for Assessing Forest Soil Nitrogen Availability. Soil Sci. Soc. Am. J. 47, 1050–1052.
Buma, B., Brown, C.D., Donato, D.C., Fontaine, J.B., Johnstone, J.F., 2013. The Impacts of Changing Disturbance Regimes on Serotinous Plant Populations and Communities. Bioscience 63, 866–876.
Busby, S.U., Holz, A., 2022. Interactions Between Fire Refugia and Climate-Environment Conditions Determine Mesic Subalpine Forest Recovery After Large and Severe Wildfires. Frontiers in Forests and Global Change 5.
Carlson, A.R., Sibold, J.S., Negrón, J.F., 2020a. Canopy structure and below-canopy temperatures interact to shape seedling response to disturbance in a Rocky Mountain subalpine forest. For. Ecol. Manage. 472, 118234.
Carlson, A.R., Sibold, J.S., Negrón, J.F., 2020b. Wildfire and spruce beetle outbreak have mixed effects on below-canopy temperatures in a Rocky Mountain subalpine forest. Journal of Biogeography:jbi.13994.
Certini, G., 2005. Effects of fire on properties of forest soils: a review. Oecologia 143, 1–10.
Chambers, M.E., Fornwalt, P.J., Malone, S.L., Battaglia, M.A., 2016. Patterns of conifer regeneration following high severity wildfire in ponderosa pine – dominated forests of the Colorado Front Range. For. Ecol. Manage. 378, 57–67.
Clark, J.S., Andrus, R., Aubry-Kientz, M., Bergeron, Y., Bogdziewicz, M., Bragg, D.C., Brockway, D., Cleavitt, N.L., Cohen, S., Courbaud, B., Daley, R., Das, A.J., Dietze, M., Fahey, T.J., Fer, I., Franklin, J.F., Gehring, C.A., Gilbert, G.S., Greenberg, C.H., Guo, Q., HilleRisLambers, J., Ibanez, I., Johnstone, J., Kilner, C.L., Knops, J., Koenig, W.D., Kunstler, G., LaMontagne, J.M., Legg, K.L., Luongo, J., Lutz, J.A., Macias, D., McIntire, E.J.B., Messaoud, Y., Moore, C.M., Moran, E., Myers, J.A., Myers, O.B., Nunez, C., Parmenter, R., Pearse, S., Pearson, S., Poulton-Kamakura, R., Ready, E., Redmond, M.D., Reid, C.D., Rodman, K.C., Scher, C.L., Schlesinger, W.H., Schwantes, A.M., Shanahan, E., Sharma, S., Steele, M.A., Stephenson, N.L., Sutton, S., Swenson, J.J., Swift, M., Veblen, T.T., Whipple, A.V., Whitham, T.G., Wion, A.P., Zhu, K., Zlotin, R., 2021. Continent-wide tree fecundity driven by indirect climate effects. Nat. Commun. 12, 1242.
Coop, J.D., Delory, T.J., Downing, W.M., Haire, S.L., Krawchuk, M.A., Miller, C., Parisien, M.A., Walker, R.B., 2019. Contributions of fire refugia to resilient ponderosa pine and dry mixed-conifer forest landscapes. Ecosphere 10, e02809.
Coop, J.D., Parks, S.A., Stevens-Rumann, C.S., Crausbay, S.D., Higuera, P.E., Hurteau, M. D., Tepley, A., Whitman, E., Assal, T., Collins, B.M., Davis, K.T., Dobrowski, S., Falk, D.A., Fornwalt, P.J., Fulé, P.Z., Harvey, B.J., Kane, V.R., Littlefield, C.E., Margolis, E.Q., North, M., Parisien, M.A., Prichard, S., Rodman, K.C., 2020. Wildfire-Driven Forest Conversion in Western North American Landscapes. Bioscience 70, 659–673.
Crockett, J.L., Hurteau, M.D., 2022. Post-fire early successional vegetation buffers surface microclimate and increases survival of planted conifer seedlings in the southwestern United States. Can. J. For. Res. 52, 416–425.
Davis, K.T., Dobrowski, S.Z., Higuera, P.E., Holden, Z.A., Veblen, T.T., Rother, M.T., Parks, S.A., Sala, A., Maneta, M.P., 2019a. Wildfires and climate change push low-elevation forests across a critical climate threshold for tree regeneration. Proc. Natl. Acad. Sci. 116, 6193–6198.
Davis, K.T., Dobrowski, S.Z., Holden, Z.A., Higuera, P.E., Abatzoglou, J.T., 2019b. Microclimatic buffering in forests of the future: the role of local water balance. Ecography 42, 1–11.
Davis, K.T., Higuera, P.E., Dobrowski, S., Parks, S., Abatzoglou, J.T., Rother, M., Veblen, T., 2020. Fire-catalyzed vegetation shifts in ponderosa pine and Douglas-fir forests of the western United States. Environ. Res. Lett. 15, 1040–1048.
Davis, K.T., Higuera, P.E., Sala, A., 2018. Anticipating fire-mediated impacts of climate change using a demographic framework. Funct. Ecol. 32, 1729–1745.

De Frenne, P., Zellweger, F., Rodríguez-Sánchez, F., Scheffers, B.R., Hylander, K., Luoto, M., Vellend, M., Verheyen, K., Lenoir, J., 2019. Global buffering of temperatures under forest canopies. Nat. Ecol. Evol. 3, 744–749.
Dobrowski, S.Z., 2011. A climatic basis for microrefugia: the influence of terrain on climate. Glob. Change Biol. 17, 1022–1035.
Donato, D.C., Harvey, B.J., Turner, M.G., 2016. Regeneration of montane forests 24 years after the 1988 Yellowstone fires: A fire-catalyzed shift in lower treelines? Ecosphere 7, e01410.
Enright, N.J., Fontaine, J.B., Bowman, D.M.J.S., Bradstock, R.A., Williams, R.J., 2015. Interval squeeze: Altered fire regimes and demographic responses interact to threaten woody species persistence as climate changes. Front. Ecol. Environ. 13.
Falk, D.A., van Mantgem, P.J., Keeley, J.E., Gregg, R.M., Guiterman, C.H., Tepley, A.J., Young, D.J.N., Marshall, L.A., 2022. Mechanisms of forest resilience. For. Ecol. Manage. 512, 120129.
Fox, J., Weisberg, S., 2018. Visualizing fit and lack of fit in complex regression models with predictor effect plots and partial residuals. J. Stat. Softw. 87.
Fukami, T., 2015. Historical Contingency in Community Assembly: Integrating Niches, Species Pools, and Priority Effects. Annu. Rev. Ecol. Evol. Syst. 46, 1–23.
Gill, N.S., Jarvis, D., Veblen, T.T., Pickett, S.T.A., Kulakowski, D., 2017. Is initial post-disturbance regeneration indicative of longer-term trajectories? Ecosphere 8, e01924.
Gill, N.S., Turner, M.G., Brown, C.D., Glassman, S.I., Haire, S.L., Hansen, W.D., Pansing, E.R., St Clair, S.B., Tomback, D.F., 2022. Limitations to Propagule Dispersal Will Constrain Postfire Recovery of Plants and Fungi in Western Coniferous Forests. BioScience:biab139.
Gunderson, L.H., 2000. Ecological Resilience—In Theory and Application. Annu. Rev. Ecol. Syst. 31, 425–439.
Halofsky, J.S., Donato, D.C., Franklin, J.F., Halofsky, J.E., Peterson, D.L., Harvey, B.J., 2018. The nature of the beast: examining climate adaptation options in forests with stand-replacing fire regimes. Ecosphere 9, e02140.
Hankin, L.E., Higuera, P.E., Davis, K.T., Dobrowski, S.Z., 2018. Accuracy of node and bud-scar counts for aging two dominant conifers in western North America. For. Ecol. Manage. 427, 365–371.
Hansen, W.D., Braziunas, K.H., Rammer, W., Seidl, R., Turner, M.G., 2018. It takes a few to tango: changing climate and fire regimes can cause regeneration failure of two subalpine conifers. Ecology 99, 966–977.
Hartig, F., 2021. Residual Diagnostics for Hierarchical (Multi-Level / Mixed) Regression Models [R package DHARMa version 0.4.1]. Comprehensive R Archive Network (CRAN).
Harvey, B.J., Donato, D.C., Turner, M.G., 2016a. Drivers and trends in landscape patterns of stand-replacing fire in forests of the US Northern Rocky Mountains (1984–2010). Landscape Ecol.
Harvey, B.J., Donato, D.C., Turner, M.G., 2016b. High and dry: post-fire tree seedling establishment in subalpine forests decreases with post-fire drought and large stand-replacing burn patches. Glob. Ecol. Biogeogr. 25, 655–669.
Hill, E.M., Ex, S., 2020. Microsite conditions in a low-elevation Engelmann spruce forest favor ponderosa pine establishment during drought conditions. For. Ecol. Manage. 463, 118037.
Hoecker, T.J., Hansen, W.D., Turner, M.G., 2020. Topographic position amplifies consequences of short-interval stand-replacing fires on postfire tree establishment in subalpine conifer forests. For. Ecol. Manage. 478, 118523.
Hoecker, T.J., Turner, M.G., 2022. A short-interval reburn catalyzes departures from historical structure and composition in a mesic mixed-conifer forest. For. Ecol. Manage. 504, 119814.
Holden, Z.A., Swanson, A., Luce, C.H., Jolly, W.M., Maneta, M., Oyler, J.W., Warren, D. A., Parsons, R., Affleck, D., 2018. Decreasing fire season precipitation increased recent western US forest wildfire activity. Proc. Natl. Acad. Sci. 115, E8349–E8357.
Holden, Z., Warren, A., Jungck, E., Maneta, M., Dobrowski, S., Davis, K., Archer, V., Fox, S., 2021. Topofire – Regeneration Mapper. University of Montana, Missoula.
Isaac, L.A., Hopkins, H.G., 1937. The Forest Soil of the Douglas Fir Region, and Changes Wrought Upon it by Logging and Slash Burning. Ecology 18, 264–279.
Johnson, D.M., McCulloh, K.A., Reinhardt, K., 2011. The Earliest Stages of Tree Growth: Development, Physiology and Impacts of Microclimate. In: Meinzer, F.C., Lachenbruch, B., Dawson, T.E. (Eds.), Size- and Age-Related Changes in Tree Structure and Function. Springer, Netherlands, Dordrecht, Netherlands, pp. 65–87.
Johnstone, J.F., Allen, C.D., Franklin, J.F., Frelich, L.E., Harvey, B.J., Higuera, P.E., Mack, M.C., Meentemeyer, R.K., Metz, M.R., Perry, G.L.W., Schoennagel, T., Turner, M.G., 2016. Changing disturbance regimes, ecological memory, and forest resilience. Front. Ecol. Environ. 14, 369–378.
Johnstone, J.F., Chapin, F.S., 2006. Effects of Soil Burn Severity on Post-Fire Tree Recruitment in Boreal Forest. Ecosystems 9, 14–31.
Karavani, A., Boer, M.M., Baudena, M., Colinas, C., Díaz-Sierra, R., Pemán, J., de Luis, M., Enríquez-de-Salamanca, Á., Resco de Dios, V., 2018. Fire-induced deforestation in drought-prone Mediterranean forests: drivers and unknowns from leaves to communities. Ecol. Monogr. 88, 141–169.
Kemp, K.B., Higuera, P.E., Morgan, P., 2016. Fire legacies impact conifer regeneration across environmental gradients in the U.S. northern Rockies. Landscape Ecol. 31, 619–636.
Kemp, K.B., Higuera, P.E., Morgan, P., Abatzoglou, J.T., 2019. Climate will increasingly determine post-fire tree regeneration success in low-elevation forests, Northern Rockies, USA. Ecosphere 10, e02568.
Keyes, C. R., R. Manso Gonzalez, and R. M. Gonzalez. 2015. Climate-influenced ponderosa pine (Pinus ponderosa) seed masting trends in western Montana, USA.
Kolb, P.F., Robberecht, R., 1996. High temperature and drought stress effects on survival of Pinus ponderosa seedlings. Tree Physiol. 16, 665–672.
Kolb, T.E., Flathers, K., Bradford, J.B., Andrews, C., Asherin, L.A., Moser, W.K., 2020. Stand Density, Drought and Herbivory Constrain Ponderosa Pine Regeneration Pulse. Canadian Journal of Forest. Research:cjfr-2019-0248.
Landhausser, S.M., Stadt, K.J., Lieffers, V.J., 1996. Screening for Control of a Forest Weed: Early Competition Between Three Replacement Species and Calamagrostis canadensis of Picea glauca. J. Appl. Ecol. 33, 1517–1526.
Littlefield, C.E., 2019. Topography and post-fire climatic conditions shape spatio-temporal patterns of conifer establishment and growth. Fire. Ecology 15.
Ma, S., Concilio, A., Oakley, B., North, M., Chen, J., 2010. Spatial variability in microclimate in a mixed-conifer forest before and after thinning and burning treatments. For. Ecol. Manage. 259, 904–915.
McCune, B., Keon, D., 2002. Equations for potential annual direct incident radiation and heat load. J. Veg. Sci. 13, 603–606.
Miller, M.L., Johnson, D.M., 2017. Vascular development in very young conifer seedlings: Theoretical hydraulic capacities and potential resistance to embolism. Am. J. Bot. 104, 979–992.
Minore, D., 1979. Comparative autoecological characteristics of northwestern tree species - a literature review. Portland, OR.
Morgan, P., Heyerdahl, E.K., Gibson, C.E., 2008. Multi-season climate synchronized fires throughout the 20th century, northern Rockies, USA. Ecology 89, 717–728.
MTBS Project (USDA Forest Service/U.S. Geological Survey). 2019. MTBS Data Acces: Fire Level Geospatial Data. http://mtbs.gov.
Nilsen, P., 1995. Effect of nitrogen on drought strain and nutrient uptake in Norway spruce Picea abies (L.) Karst.) trees. Plant Soil 172, 73–85.
Parks, S.A., Abatzoglou, J.T., 2020. Warmer and Drier Fire Seasons Contribute to Increases in Area Burned at High Severity in Western US Forests From 1985 to 2017. Geophys. Res. Lett. 47:e2020GL089858.
Parra, A., Moreno, J.M., 2017. Post-fire environments are favourable for plant functioning of seeder and resprouter Mediterranean shrubs, even under drought. New Phytol. 214, 1118–1131.
Pausas, J.G.G., Ouadah, N., Ferran, A., Gimeno, T., Vallejo, R., 2002. Fire severity and seedling establishment in Pinus halepensis woodlands, eastern Iberian Peninsula. Plant Ecol. 169, 205–213.
Peeler, J.L., Smithwick, E.A.H., 2020. Seed source pattern and terrain have scale-dependent effects on post-fire tree recovery. Landscape Ecol. 35, 1945–1959.
Plamboeck, A.H., North, M., Dawson, T.E., 2008. Conifer Seedling Survival Under Closed-Canopy And Manzanita Patches In the Sierra Nevada. Madroño 55, 191–201.
Povak, N.A., Churchill, D.J., Cansler, C.A., Hessburg, P.F., Kane, V.R., Kane, J.T., Lutz, J. A., Larson, A.J., 2020. Wildfire severity and postfire salvage harvest effects on long-term forest regeneration. Ecosphere 11.
Prichard, S.J., Hessburg, P.F., Hagmann, R.K., Povak, N.A., Dobrowski, S.Z., Hurteau, M. D., Kane, R.V., Keane, R.E., Kobziar, L.N., Kolden, C.A., North, M., Parks, S.A., Safford, H.D., Stevens, J.T., Yocom, L.L., Churchill, D.J., Gray, R.W., Huffman, D.W., Lake, F.K., Khatri-Chhetri, P., 2021. Adapting western North American forests to climate change and wildfires: ten common questions. Ecological. Applications: e02433.
PRISM Climate Group (Oregon State University). 2015. PRISM 30-Year Normals. Oregon State University. http://prism.oregonstate.edu.
R Core Team, 2020. R: A language and environment for statistical computing. R Foundation for Statistical Computing, Vienna, Austria.
Rammer, W., Braziunas, K.H., Hansen, W.D., Ratajczak, Z., Westerling, A.L., Turner, M. G., Seidl, R., 2021. Widespread regeneration failure in forests of Greater Yellowstone under scenarios of future climate and fire. Glob. Change Biol. 00:gcb.15726.
Remke, M.J., Hoang, T., Kolb, T., Gehring, C., Johnson, N.C., Bowker, M.A., 2020. Familiar soil conditions help Pinus ponderosa seedlings cope with warming and drying climate. Restor. Ecol. 28, S344–S354.
Robin, X., N. Turck, A. Hainard, N. Tiberti, F. Lisacek, J. Sanchez, and M. Muller. 2011. pROC: an open-source package for R and S+ to analyze and compare ROC curves.
Rodman, K.C., Veblen, T.T., Battaglia, M.A., Chambers, M.E., Fornwalt, P.J., Holden, Z. A., Kolb, T.E., Ouzts, J.R., Rother, M.T., 2020a. A changing climate is snuffing out post-fire recovery in montane forests. Global Ecology and. Biogeography.
Rodman, K.C., Veblen, T.T., Chapman, T.B., Rother, M.T., Wion, A.P., Redmond, M.D., 2020b. Limitations to recovery following wildfire in dry forests of southern Colorado and northern New Mexico, USA. Ecol. Appl. 30, e02001.
Smithwick, E.A.H., Turner, M.G., Mack, M.C., Chapin, F.S., 2005. Postfire Soil N Cycling in Northern Conifer Forests Affected by Severe, Stand-Replacing Wildfires. Ecosystems 8, 163–181.
Soil Survey Staff, 2017. SSURGO Web Soil Survey. Natural Resources Conservation Service, USDA.
Steed, J.E., Goeking, S.A., 2020. Western larch regeneration responds more strongly to site and indirect climate factors than to direct climate factors. Forests 11.
Stein, S.J., Kimberling, D.N., 2003. Germination, establishment, and mortality of naturally seeded Southwestern ponderosa pine. West. J. Appl. For. 18, 109–114.
Stevens-Rumann, C.S., Kemp, K.B., Higuera, P.E., Harvey, B.J., Rother, M.T., Donato, D. C., Morgan, P., Veblen, T.T., 2018. Evidence for declining forest resilience to wildfires under climate change. Ecol. Lett. 21, 243–252.
Stevens-Rumann, C.S., Morgan, P., 2019, December 1. Tree regeneration following wildfires in the western US: a review. SpringerOpen.
Stewart, J.A.E., van Mantgem, P.J., Young, D.J.N., Shive, K.L., Preisler, H.K., Das, A.J., Stephenson, N.L., Keeley, J.E., Safford, H.D., Wright, M.C., Welch, K.R., Thorne, J. H., 2021. Effects of postfire climate and seed availability on postfire conifer regeneration. Ecol. Appl. 31, e02280.
Taudière, A., Richard, F., Carcaillet, C., 2017. Review on fire effects on ectomycorrhizal symbiosis, an unachieved work for a scalding topic. For. Ecol. Manage. 391, 446–457.

Tepley, A.J., Swanson, F.J., Spies, T.A., 2013. Fire-mediated pathways of stand development in Douglas-fir/western hemlock forests of the Pacific Northwest, USA. Ecology 94, 1729–1743.
Tepley, A.J., Thompson, J.R., Epstein, H.E., Anderson-Teixeira, K.J., 2017. Vulnerability to forest loss through altered postfire recovery dynamics in a warming climate in the Klamath Mountains. Glob. Change Biol. 23, 4117–4132.
Turner, M.G., Braziunas, K.H., Hansen, W.D., Harvey, B.J., 2019. Short-interval severe fire erodes the resilience of subalpine lodgepole pine forests. PNAS 166, 11319–11328.
Turner, M.G., Hargrove, W.W., Gardner, R.H., Romme, W.H., 1994. Effects of fire on landscape heterogeneity in Yellowstone National Park, Wyoming. J. Veg. Sci. 5, 731–742.
Turner, M.G., Whitby, T.G., Tinker, D.B., Romme, W.H., 2016. Twenty-four years after the Yellowstone Fires: Are postfire lodgepole pine stands converging in structure and function? Ecology 97, 1260–1273.
Urza, A.K., Sibold, J.S., 2013. Nondestructive Aging of Postfire Seedlings for Four Conifer Species in Northwestern Montana. West. J. Appl. For. 28, 22–29.
Urza, A.K., Sibold, J.S., 2017. Climate and seed availability initiate alternate post-fire trajectories in a lower subalpine forest. J. Veg. Sci. 28, 43–56.
Urza, A.K., Weisberg, P.J., Chambers, J.C., Sullivan, B.W., 2019. Shrub facilitation of tree establishment varies with ontogenetic stage across environmental gradients. New Phytol. 223, 1795–1808.
Wagner, R.G., Petersen, T.D., Ross, D.W., Radosevich, S.R., 1989. Competition thresholds for the survival and growth of ponderosa pine seedlings associated with woody and herbaceous vegetation. New Forest. 3, 151–170.
Wang, T., Hamann, A., Spittlehouse, D., Carroll, C., 2016. Locally downscaled and spatially customizable climate data for historical and future periods for North America. PLoS ONE 11, e0156720.
Western Regional Climate Center. 2021. Western U.S. Climate Historical Summaries. NOAA.
Wolf, K.D., Higuera, P.E., Davis, K.T., Dobrowski, S.Z., 2021. Wildfire impacts on forest microclimate vary with biophysical context. Ecosphere 12, e03467.
Zellweger, F., Frenne, P.D., Lenoir, J., Vangansbeke, P., Verheyen, K., Bernhardt-Römermann, M., Baeten, L., Hédl, R., Berki, I., Brunet, J., Calster, H.V., Chudomelová, M., Decocq, G., Dirnböck, T., Durak, T., Heinken, T., Jaroszewicz, B., Kopecký, M., Máliš, F., Macek, M., Malicki, M., Naaf, T., Nagel, T.A., Ortmann-Ajkai, A., Petřík, P., Pielech, R., Reczyńska, K., Schmidt, W., Standovár, T., Świerkosz, K., Teleki, B., Vild, O., Wulf, M., Coomes, D., 2020. Forest microclimate dynamics drive plant responses to warming. Science 368, 772–775.